Tire Cornering Simulation Using Finite Element Analysis

KAZUYUKI KABE, MASATAKA KOISHI

Computational Mechanics Lab. Research and Development Center, Yokohama Rubber Co., 2-1, Oiwake, Hiratsuka, Kanagawa 254-8601, Japan

ABSTRACT: The finite element method (FEM) has been used widely in tire engineering. Most tire simulations with FEM are static analysis, because tire is one of most complex structures. Recently, transient analysis has been studied with explicit finite element analysis code. In this paper, at first, we describe characteristics of tire analysis by means of FEM, and implicit/explicit finite element codes for analysis. And then we conduct tire cornering simulation with implicit and explicit finite element analysis codes, where implicit finite element analysis (FEA) describes the steady state cornering simulation and explicit FEA describes transient cornering simulation. In the case of implicit FEA, finite element model of tire requires the fine mesh only in the contact region because of formulation by moving reference frame technique. On the other hand, for explicit FEA, fine mesh is required in the circumferential direction of tire. Predicted cornering forces of passenger car's tire using implicit/explicit FEM are compared with experimental results obtained from MTS Flat-Test Tire Test Systems. We can get a good correlation between predicted ones and experimental ones. CPU time for cornering simulation using implicit FEM is shorter than that of explicit FEM. © 2000 John Wiley & Sons, Inc. J Appl Polym Sci 78: 1566–1572, 2000

Key words: tire; cornering; finite element method

INTRODUCTION

The finite element method has been used widely in tire engineering. Since a tire is one of the most complex nonlinear structures, most finite element analysis of a tire has been limited to static analysis. Recently, transient finite element analysis of a tire has been studied using an explicit finite element code[1,2] due to the development of both finite element (FE) program and computer hardware. Although the explicit finite element analysis code is efficient for dynamic analysis of a rolling tire, it has a high CPU cost.[3]

In this paper we first describe characteristics of tire analysis by means of FE method (FEM), and implicit/explicit finite element codes for analysis.

And then we conduct tire cornering simulation with implicit and explicit finite element analysis codes, where implicit FE analysis (FEA) describes the steady state cornering simulation and explicit FEA describes transient cornering simulation. In the case of the implicit FEA, the finite element model of tire requires a fine mesh only in the contact region because of formulation by moving reference frame technique. On the other hand, for explicit FEA, fine mesh is required in the circumferential direction of tire. Predicted cornering forces of passenger car's tire using implicit/explicit FEA are compared with experimental results obtained from MTS Flat-Test Tire Test Systems.

CHARACTERISTICS OF TIRE

Basic functions required of a tire are as follows:

1. Load-carrying capacity

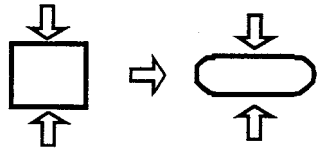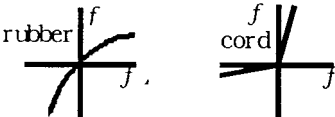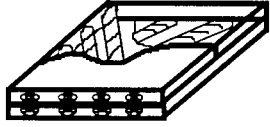2. Transmission of driving and breaking torque
3. Cushioning ability
4. Road-holding ability

In addition to the above four functions, a tire needs to have many other functions: for example, to provide steering response, adequate mileage, and dimensional stability; to consume minimum power; and to have minimum noise and vibration. In order to satisfy these many functions, a tire forms a thin-walled composite toroidal shell with rubber and cord, which is both highly flexible and relatively inextensible. Characteristics of such a tire are shown as follows (refer Table I):

- large deformation and large strain,
- incompressibility of rubber,
- material nonlinearity of rubber and cord,
- composite structure (FRR; Fiber Reinforced Rubber),
- viscoelasticity of rubber, and
- rolling contact of tire in service.
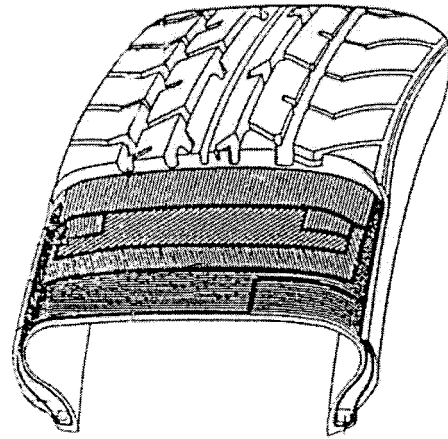
Table I   Characteristics of Tire

Figure 1   Cross-section of passenger car's radial tire.

When we apply FEM to tire analysis, these characteristics should be taken into account for the analysis of actual tire response.

FINITE ELEMENT METHOD FOR TIRE ANALYSIS

FEM has been used widely in tire engineering. Most of tire simulations with FEM are static analyses, because tires are very complex nonlinear structures. Recently, transient analysis has been studied with explicit finite element analysis code. In order to compute dynamic response of a rolling tire, two different methodologies have been proposed. One is the implicit time integration technique,[4-8] in which special kinematical relationships are used to compute steady state dynamic response of rolling tire. For example, Faria[8] shows a steady state formulation of the rolling contact problem with friction that allows analyses of free rolling, cornering, acceleration, and breaking. Another is the explicit time integration technique, e.g., LS/DYNA3D[1] and PAM-SHOCK,[2] as commercial codes. Kamoulakos and Kao[2] studied the transient dynamic responses of a tire rolling on a spinning drum with cleat.

In the following section, we also show a finite element model of tire and cornering simulation of tire using implicit FEA code (ABAQUS/Standard) and explicit FEA code (ABAQUS/Explicit).

FINITE ELEMENT MODEL OF TIRE

Figure 1 shows a structure of the typical passenger car's radial tire. The tire is made of both
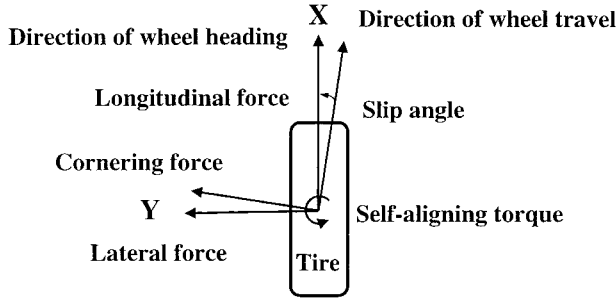
Figure 2 Coordinate system of tire.

rubber components such as cap tread and sidewall, and fiber-reinforced rubber components such as steel belt and textile carcass.

Figure 2 shows an axis system for this simulation. A slip angle is an angle between direction of wheel travel and direction of wheel heading. A cornering force and a self-aligning torque characterize cornering ability of a tire. Direction of the cornering force is normal to direction of wheel travel. The self-aligning torque is moment around the axis in the direction of normal to road surface.

Figure 3 shows an axisymmetric FE tire model, which is a passenger car's radial tire of 235/45ZR17. Rubber components are modeled by the continuous elements with hyperelastic material of Mooney–Rivlin form. The hybrid axisymmetric continuous element with twist degree of freedom is useful for tire modeling. Although a tire is axisymmetric geometry, the inflated tire becomes twist along the axisymmetric axis due to anisotropy of fiber reinforcements. Fiber reinforcement is modeled by the REBAR, which is embedded in the continuous elements, with linear elastic material.

Since an angle and a spacing of fiber reinforcements are changed during manufacturing process, the angle and the spacing of REBAR at each

location in a cross-section of tire should be determined using following lift equations. Assuming a deformation during manufacturing process is purely due to pantographic action, the angle and spacing of REBAR in the cured tire can be obtained as follows:

$$\alpha = \left[\frac{r' \sin \beta'}{r \sin \beta}\right]\alpha', \quad \beta = \cos^{-1}\left[\frac{r \cos \beta'}{r'(1 + \varepsilon)}\right] \quad (1)$$

where α, β, r, and ε are spacing, angle, radius, and elongation factor of fiber reinforcements after lift, respectively. Also, α', β', and r' are spacing, angle, and radius on a tire-building drum. After a tire is mounted on a rim, an inflation pressure of 200 kPa is applied to the axisymmetric tire FE model.

Tire Model for Implicit FEA

Figure 4 shows a three-dimensional FE tire model that can be generated based on the inflated results with the symmetric model generation, and the symmetric results are transferred to a three-dimensional format with capability of ABAQUS/Standard. A pavement is modeled as a rigid element. The steady-state transport analysis capability can be formulated with a moving reference frame technique, so a mesh needs only to be refined in a contact region, as shown in Figure 4. This model has 5976 nodes and 4464 elements. On the other hand, a fine mesh is required in circumferential direction for the explicit finite element technique, as mentioned later.[3]

Before a cornering simulation of a tire, braking and driving simulations are conducted with slip angle of 0° in order to determine a free rolling radius of a tire. In the steady-state rolling simulation based on moving reference frame tech-
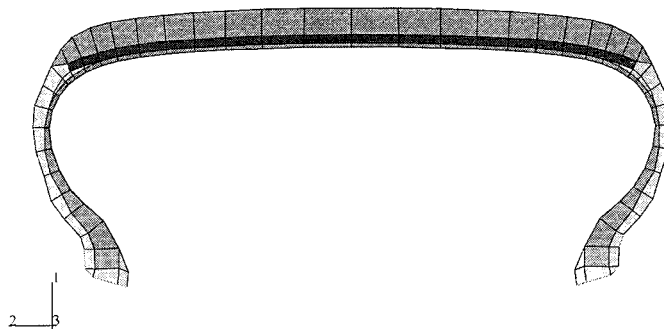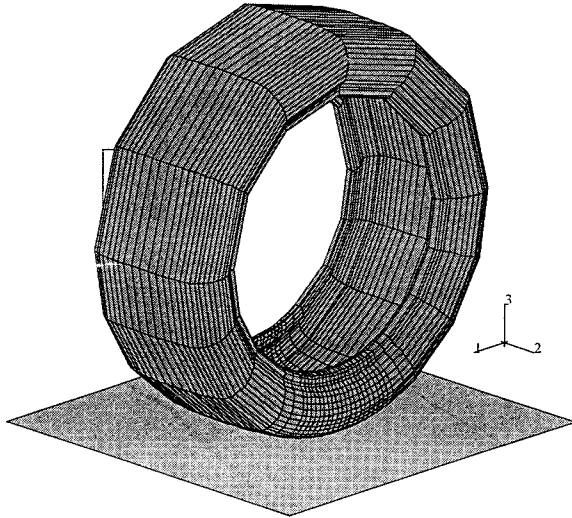

Figure 3 Axisymmetric FE tire.

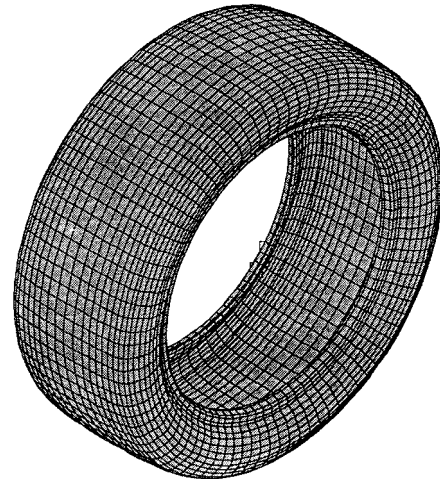**Figure 4** Three-dimensional tire model for implicit FEA.

Figure 6 Three-dimensional tire model for explicit FEA.

nique, angular velocity of a tire is required to synchronize with travel velocity. The free rolling radius of a tire can be determined from the braking and driving simulations. Free rolling is defined as the state at which no longitudinal force occurs.

The tire model is in contact with a road under vertical load of 4 kN traveling at 10 km/h. Angular velocity of the tire is varied from 8 to 10 rad/s in order to determine the free rolling radius. Figure 5 shows the driving force of the tire (referred to as longitudinal force) at different angular velocities. It is shown that free rolling occurs at angular velocity of 8.87 rad/s. Therefore, we can estimate the free rolling radius of 313.28 mm.
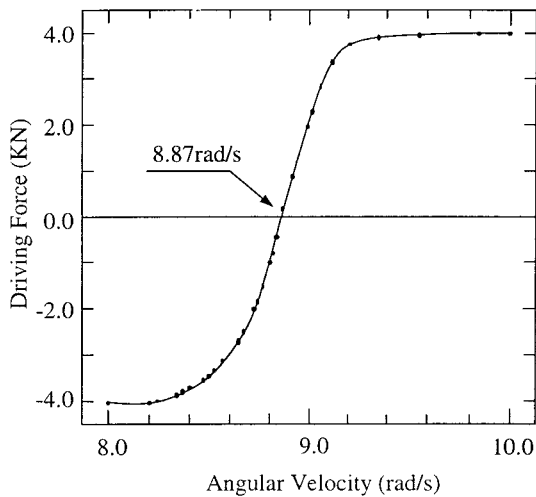

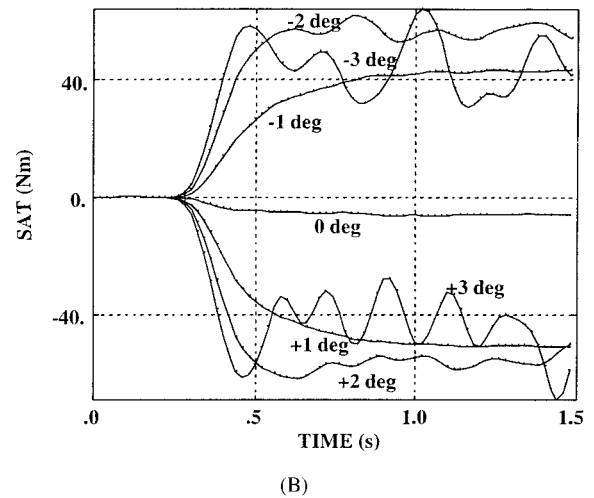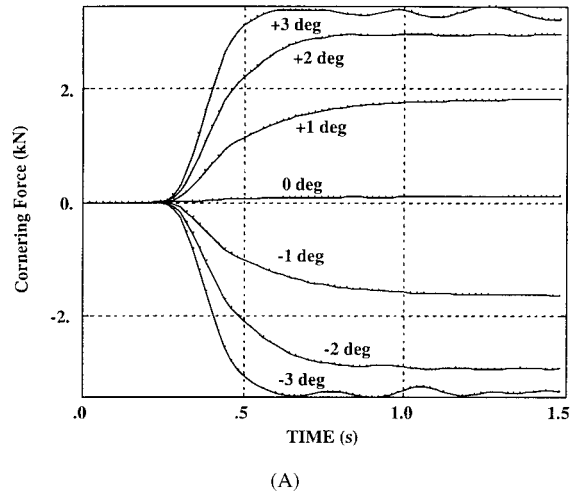**Figure 5** Driving force vs angular velocity of tire.

(A)

(B)

Figure 7 (A) Transient results of cornering force. (B) Transient results of self aligning torque.
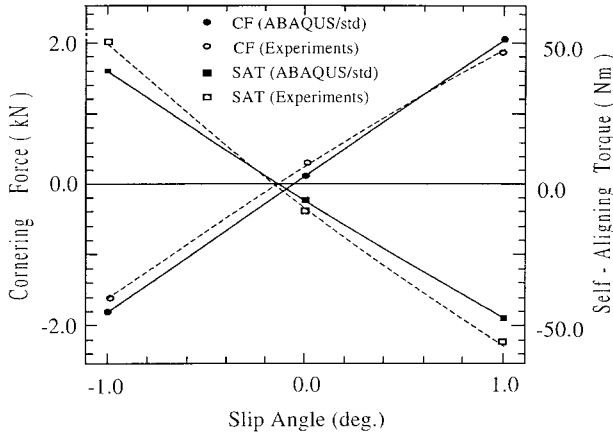
Figure 8   Cornering force and self aligning torque.

TIRE MODEL FOR EXPLICIT FEA

Figure 6 shows a three-dimensional FE tire model by means of the same procedure as mentioned above. In the case of explicit FEA, the FE tire model must have a fine mesh (14,940 nodes, 11,160 elements) all over the circumferential direction in order to analyze a transit response of a tire. This causes more numbers of element and node than in case of the implicit FEA. Also, three-dimensional FEA must be needed not only for a rolling analysis, but also for an inflation analysis. These cause to spend longer CPU times than in the case of the implicit FEA.

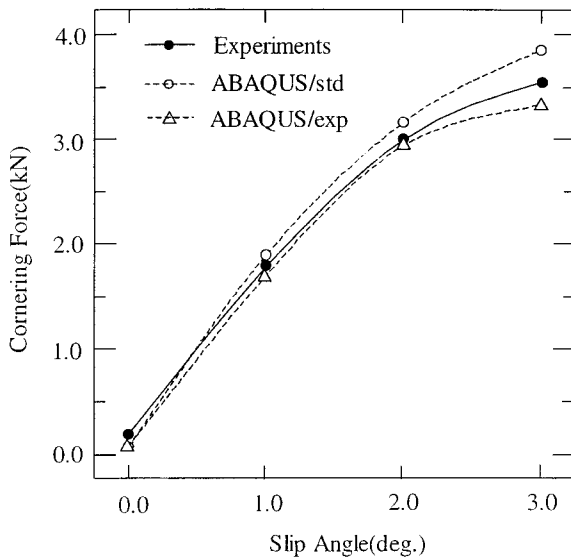Figure 7(A) and (B) show examples of time history for computed CF (cornering force) and
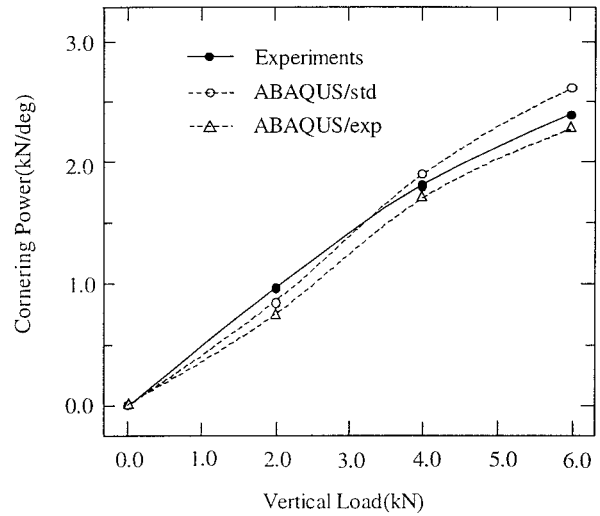

Figure 10   Cornering power at various vertical loads.

SAT (Self-Aligning Torque) using explicit FEM. From these figures, external loads and external moments (torque) are applied for 0.25 s, and then each force and moment remain constant with time. We define the computed CF and SAT as a mean value of this stable region.

CORNERING SIMULATION

Cornering simulation is conducted at seven different slip angles such as 0°, ±1°, ±2°, and ±3°
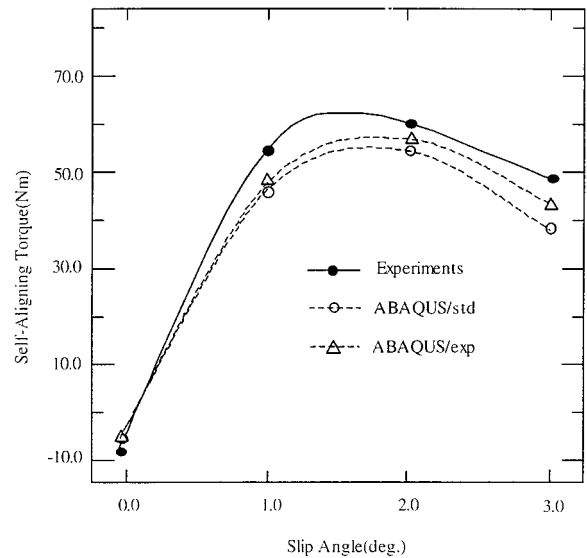

Figure 9   Cornering force at various slip angles.

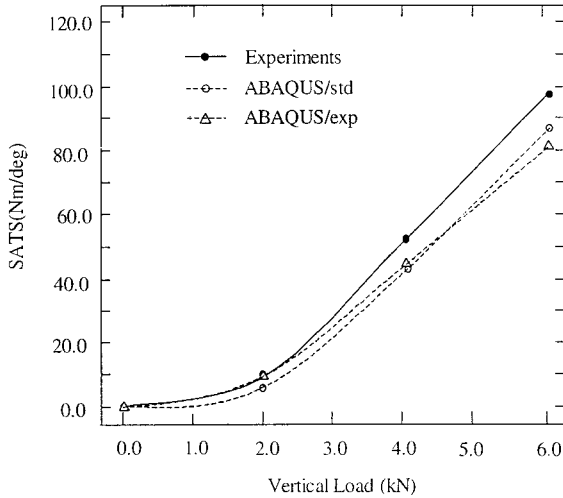**Figure 11**   Self-aligning torque at various slip angles.

Figure 12   Self-aligning torque stiffness.

with inflation pressure (P) of 200 MPa, vertical load (W) of 4 kN, and velocity (V) of 10 km/h.

Figure 8 shows predicted CF and SAT at slip angles of $-1°$, $0°$, and $1°$, which are simulated using implicit FEM. In this figure, experimental results are obtained using the MTS Flat-Track Tire Test Systems. From this figure, nonzero CF and SAT are obtained at slip angle of $0°$ on both finite element analysis and experiment. These are caused by ply steer force due to anisotropy of steel belt. The calculated results agree well with the experimental results.

Figure 9 shows predicted CF at various slip angles using implicit and explicit FEM, together with the experimental results, which are between results of implicit and explicit FEM. The numerical and experimental results shown in this figure are averaged value between ones at negative slip angle and at positive slip angle. The calculated results agree well with the experimental results.

Figure 10 shows cornering power at various vertical loads using implicit and explicit FEM, together with the experimental results. The cornering power is defined as cornering force at slip angle of $1°$. The calculated results agree well with the experimental results.

Figure 11 shows SAT at various slip angle using implicit and explicit FEM, together with the experimental results, which are larger than both calculated SAT.

Figure 12 shows SATS (Self-Aligning Torque Stiffness) at various vertical loads using implicit and explicit FEM, together with the experimental results. The SATS is defined as the self-aligning torque at slip angle of $1°$. This figure shows good correlation between calculated results and experimental ones.

Also, Figure 13 shows contact shapes and contact pressure distributions at slip angle of $3°$ using both implicit and explicit FEM, respectively. From this figure, both contact shapes and contact pressure distributions have the same tendency, i.e., the maximum pressure distributions occur at shoulder area of tire tread.

Table 2 shows the CPU times in this simulation with four conditions ($0°$, $1°$, $2°$, $3°$) with a vector computer of Fujitsu VX-2. CPU times for
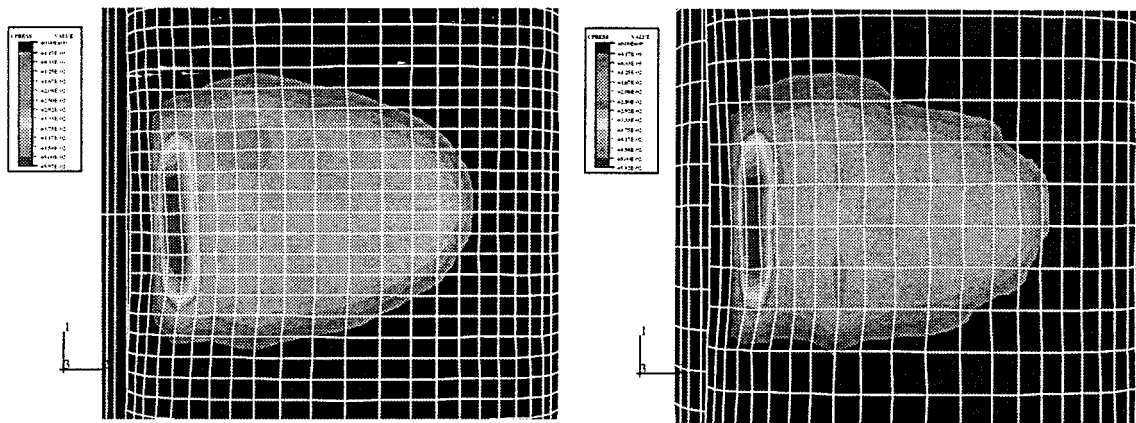
Longitudinal direction

Figure 13   Contact pressure distribution at slip angle.

Table II   CPU Time

FEA	CPU Time (Fujitsu VXE)
Implicit FEA (ABAQUS/Std.)	6.5 h
Explicit FEA (ABAQUS/Exp.)	192.0 h

the implicit FEA and explicit FEA were 6.5 and 192 h, respectively. Obviously, the CPU time of implicit FEA is about 30 times shorter than that of explicit FEA.

CONCLUSION

Cornering simulation of a tire is shown using both implicit and explicit finite element analysis codes. The computed cornering forces of tire using both implicit and explicit finite element analysis agree well with experimental results. In comparison between implicit and explicit finite element analysis, the CPU times of implicit finite element analysis is about 30 times shorter than that of explicit finite element analysis.

REFERENCES

1. Kao, B. G.; Muthukrishnan, M. Tire Sci Technol 1997, 25(4), 230.
2. Kamoulakos, A.; Kao, B. G. Tire Sci Technol 1998, 26(2), 84.
3. Koishi, M.; Kabe, K.; Shiratori, M. Tire Sci Technol 1998, 26(2), 109.
4. Padovan, J. Comput Struct 1987, 27(2), 249.
5. Kennedy, R.; Padovan, J. Comput Struct 1987, 27(2), 259.
6. Nakajima, Y.; Padovan, J. Comput Struct 1987, 27(2), 275.
7. Oden, J. T.; Lin, T. L. Comp Methods App Mechan Eng 1986, 57, 297.
8. Faria, L. O. Ph.D. dissertation, The University of Texas at Austin, 1989.
9. Sakai, H. Tire Engineering; Guranpuri Syupan, 1987 (in Japanese).